Aqueous self-assembly of pullulan-*b*-poly(2-ethyl-2-oxazoline) double hydrophilic block copolymers

Jochen Willersinn, Bernhard V. K. J. Schmidt

The self-assembly of a novel double hydrophilic block copolymer, namely pullulan-b-poly(2-ethyl-2-oxazoline), is described. Importantly, no external triggers are needed to form self-assembled structures leading to completely water-drained polymer particles. A significant effect of individual block molecular weights on the self-assembly efficiency is observed.

Aqueous self-assembly of pullulan-*b*-poly(2-ethyl-2-oxazoline) double hydrophilic block copolymers

Jochen Willersinn,[†] Bernhard V.K.J. Schmidt[†*]

[†] Max-Planck Institute of Colloids and Interfaces; Department of Colloid Chemistry, Am Mühlenberg 1, 14476 Potsdam, Germany

Correspondence to: Bernhard V.K.J. Schmidt (E-mail: bernhard.schmidt@mpikg.mpg.de)

((Additional Supporting Information may be found in the online version of this article.))

ABSTRACT

The self-assembly of a novel double hydrophilic block copolymer in water without the application of external triggers is described, namely pullulan-*b*-poly(2-ethyl-2-oxazoline) (Pull-*b*-PEtOx). The biomacromolecules Pull (8-38 kg mol^{-1}) is modified and conjugated to biocompatible PEtOx (22 kg mol^{-1}) via modular conjugation. Moreover, the molecular weight of the Pull blocks are varied to investigate the effect of molecular weight on the self-assembly behavior. Spherical particles with sizes between 300 and 500 nm are formed in diluted aqueous solution (0.1 to 1.0 wt.%) as observed via dynamic light scattering and static light scattering. Additionally, cryo scanning electron microscopy and laser scanning confocal microscopy are performed to support the finding from light scattering. The block ratio study shows an optimum ratio of Pull and PEtOx of 0.4/0.6 for self-assembly in water in the concentration range of 0.1-1.0 wt.%. At higher concentrations of 20 wt.% vesicular structures with sizes above 1 μm can be observed via optical microscopy.

INTRODUCTION

Self-assembly of various amphiphiles such as lipids and block copolymers in selective solvents is known to lead to the formation of spherical structures e.g. micelles, particles or vesicles.[1,2] The structural outcome of the self-assembly depends on several properties of the amphiphiles such as the ratio between hydrophobic and hydrophilic part, chain rigidity and the curvature between the hydrophobic-hydrophilic interface.[1,3] Vesicles based on amphiphilic block copolymers – the so-called polymersomes – have been investigated in polymer science frequently due to vast potential applications, e.g. in drug-delivery,[4,5] as nano reactors[6,7] or sensors.[8] Particularly, biomacromolecules have been utilized in that regard, e.g. poly(saccharides) like dextran,[9] poly(lactic acid)[10] or proteins.[11] Recently, control over polymersome morphology has been in the focus of research.[12,13] Therefore, shape anisotropic particles are of interest that can be generated via various methods including polymerization induced self-assembly[14] or out-of-equilibrium self-assembly.[15] Furthermore, external factors for instance a rapid change in temperature can lead to variations in the morphology of vesicular structures.[16] In that regard Mui et al. demonstrated various vesicular morphologies with rotational symmetry such as spheres and tubes.[3] Zhang et al. showed that the addition of salt or acid can have tremendous effects of the morphological shape of poly(styrene)-*b*-poly(acrylic acid) block copolymers.[17]

A recent development in polymer self-assembly is the utilization of purely double hydrophilic block copolymers (DHBCs) for the formation of particle structures in aqueous solution. In order to obtain such self-assembled structures, the

individual blocks in the DHBC have to be chosen carefully and usually high polymer concentrations have to be applied. One block has to feature a significantly higher hydrophilicity compared to the other block. Moreover, the less hydrophilic block has to be water-soluble as well to obtain complete hydrophilic structures. A phase separation can occur due to differences in concentration of the polymer blocks on the microscopic scale as the osmotic pressure has to be balanced. As shown by Brosnan et al. the formation of self-assembled structures relies significantly on polymer concentration and the polymer interfaces scale in the order of tens of nanometers.[18] Therefore, giant vesicles were formed from polysaccharide-based DHBCs at concentrations above 10 wt.%, namely pullulan-*b*-PEO and dextran-*b*-PEO.[18] Certainly, no phase transition from the hydrophilic coil to the hydrophobic globule state can be utilized in pure DHBC self-assembly as the case of solubility switches rather lead to amphiphilic systems,[19] e.g. in the case of poly(*N*-isopropylacrylamide)[20,21] or poly(*N*,*N*-diethylacrylamide).[22,23] In the case of pure DHBC self-assembly a reasonable number of examples exist in the literature, e.g. poly(2-methyl-2-oxazoline)-*b*-poly(ethylene oxide)[24,25] or poly(*N*,*N*-dimethylacrylamide)-*b*-poly(ethylene oxide).[26] Our team recently showed the formation of particles via self-assembly of poly(ethylene oxide)-*b*-poly(*N*-vinylpyrrolidone)[27] and poly(2-ethyl-2-oxazoline)-*b*-poly(*N*-vinylpyrrolidone) (PEtOx-*b*-PVP).[28] The formation of micelles was described by Böker and coworkers for the system poly(2-hydroxylethyl methacrylate)-*b*-poly(2-*O*-(*N*-acetyl-β-D-glucosamine)ethyl methacrylate)[29] as well as Bronich and coworkers for the system poly(ethylene oxide)-*b*-poly(methacrylic acid).[30] In the latter case micelles of the block copolymer were formed via addition of Ca^{2+} and the micellar structure utilized as template for crosslinking via amide formation. Moreover, the combination of pullulan with poly(acrylamides) has shown to be an efficient system for DHBC self-assembly.[31] A possible application for DHBC-based self-assemblies might be in the biomedical sector as completely hydrophilic and mostly biocompatible blocks are utilized. Due to the completely water-swollen structures enhanced permeability is expected, which might be useful for drug delivery or nano reactors.

In here the DHBC pullulan-*b*-PEtOx (Pull-*b*-PEtOx) is presented, which is – to the best of our knowledge - a novel block copolymer combination. Especially, poly(oxazolines) have been utilized frequently in the formation of complex structures in aqueous solution,[32] e.g. crystalline microspheres,[33] protein conjugation[34] or anisotropic hybrid materials.[35] Moreover, the high biocompatibility of poly(oxazolines) makes them ideal candidates for research in the direction of biomedical applications.[36,37] In that regard drug-delivery is a very promising direction.[38,39] As most of the poly(oxazolines) show reversible coil to globule transformation upon heating[40,41] a thorough investigation on that matter has to be performed in order to have a pure DHBC self-assembly system. The formation of DHBC-based poly(ethylene oxide)-*b*-PEtOx nanospheres was shown by Matějíček and coworkers.[42] The size could be controlled vie the preparation method but the inner-structure kept a homogenous polymer distribution in the particles. Moreover, the particles were crosslinked via a metallacarborane. In a similar way, particles from PEtOx-*b*-PVP were described by our group recently.[28] Pullulan, on the other hand does not show thermoresponsive solubility. Being a poly(saccharide) it is formed from maltotriose units that are connected via α-1,6 glycosidic connections. Moreover, pullulan is biocompatible and utilized in vast applications in the food and biomedical sector, e.g. for blood plasma substitutes,[43] food manufacturing[44] and pharmaceutical applications.[45] Commercial pullulan is a biomacromolecule that is derived from the microorganism *Aureobasidium pullulans*. The block copolymers are formed via copper(II) catalyzed azide alkyne cycloaddition (CuAAc),[46] which is a modular high efficient

technique for block conjugation that has found significant utilization in polymer chemistry.[47,48] As both building blocks are biocompatible application for self-assembled structures in the biomedical field are certainly possible. According to findings of Whitesides and coworkers Dextran, which is similar to Pull, and PEtOx form an aqueous two phase system.[49] Such a macroscopic demixing is a significant hint towards formation of self-assembled structures via DHBCs.
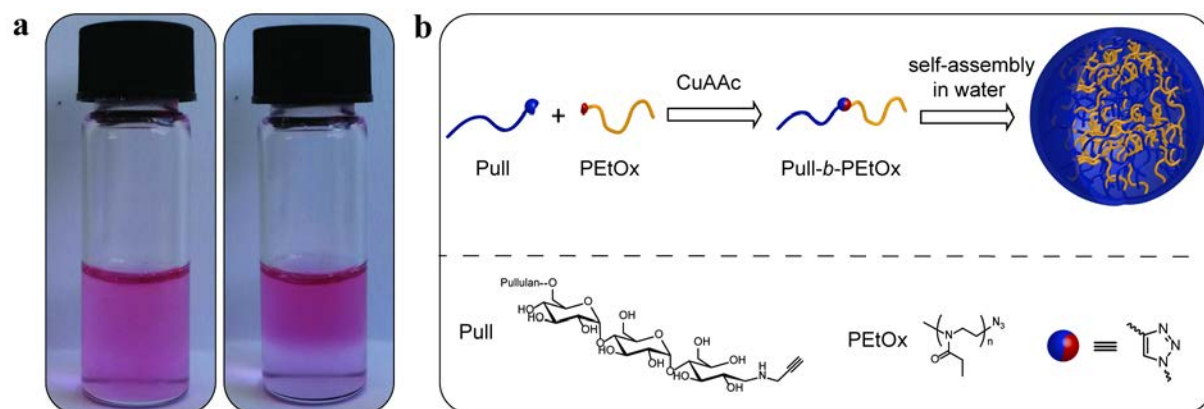
SCHEME 1 a) image of the mixture of Pull and PEtOx in water at a concentration of 10 wt.% after mixing (left) and after 5 minutes (right) at ambient temperature (a red dye was added for visualization) and b) overview of the self-assembly process of Pull-*b*-PEtOx DHBC.

Herein, the aqueous self-assembly of the novel biomacromolecule-derived DHBC Pull-*b*-PEtOx is investigated. After synthesis of individual azide or alkyne end functionalized PEtOx or Pullulan building blocks, respectively, CuAAc is utilized for the formation of block copolymers with varied molecular masses of the Pullulan block. Block copolymer formation is studied via size exclusion chromatograph (SEC) and ^{1}H NMR. Subsequently, self-assembly in water is studied with respect to the different molecular masses of the Pullulan block via dynamic light scattering (DLS) and static light scattering (SLS). Moreover, cryo scanning electron microscopy (cryo SEM) and laser scanning confocal microscopy (LSCM) are utilized to image the formed particular aggregates as well as angle dependent DLS measurements.

EXPERIMENTAL

Materials

Ascorbic acid (98%, Alfa Aesar),, $CuSO_4$ (99%, Roth KG), dimethylsulfoxide (DMSO, analytical grade, VWR Chemicals), hydrochloric acid (HCl, fuming, Roth KG), *N,N,N',N'',N''*-pentamethyldiethylenetriamine (PMDETA, 98%, Sigma Aldrich), propargyl amine (98%, Sigma Aldrich), Pluronic P-123 (pluronics, Sigma Aldrich), pullulan (TCI), Rhodamine B (Sigma Aldrich), sodium azide (>99.5%, Fluka), sodium cyanoborohydride (NaCNBH₃, 95% Sigma Aldrich). Millipore water was obtained from an Integra UV plus pure water system by SG Water (Germany). Acetate buffer was prepared via the dissolution of 30.0 g acetic acid and 41.0 g sodium acetate in 500 mL deionized water. Acetonitrile (Sigma Aldrich, 99.5%), 2-ethyl-2-oxazoline (Acros, 99%) and methyl tosylate (Fluka, 97%) were dried over CaH_2 (Acros, 93%) and distilled under argon prior to use. Azido

functionalized PS-resin, depolymerized Pullulan and alkyne-Pullulan were prepared according to the literature (refer to the SI for details, Table S1 and S2 and Figure S1).[31]

Synthesis of PEtOx$_{22k}$-N$_3$

According to the literature,[28] in a dry 250 mL ampoule methyl tosylate (152 mg, 0.82 mmol, 1.0 eq) was dissolved in dry acetonitrile (70 mL) that was cryo distilled into the ampoule. Subsequently, dry freshly distilled 2-ethyl-2-oxazoline (15 mL, 148.60 mmol, 181.2 eq) was added via syringe. The ampoule was sealed and heated to 80 °C for 3 days under stirring. After cooling down to ambient temperature sodium azide (628 mg, 9.66 mmol, 11.8 eq) was added under argon flow and the mixture stirred at 80 °C overnight. The product was precipitated into cold diethyl ether, filtered and further purified via dialysis against deionized water (MWCO 3500). The product was obtained after evaporation in vacuo as a white solid (9.35 g, 0.42 mmol, 64% recovery M_n = 22200 g·mol^{-1}, Đ= 1.24) as a white powder.

Exemplary synthesis of Pull$_{17k}$-b-PEtOx$_{22k}$

In a dry, argon purged 25 mL round bottom Schlenk flask, pullulan alkyne$_{17k}$ (0.29 g, 0.015 mmol, 1.2 eq.) was dissolved in deionized water (2.5 mL). CuSO$_4$ (1.3 mg, 8.1 µmol, 0.65 eq.) and DMSO (5.0 mL) were added to the solution. A solution of ascorbic acid (4.4 mg, 0.025 mmol, 2.0 eq.) in deionized water (2.0 mL) was added to the reaction mixture. PEtOx$_{22k}$-N$_3$ (0.25 g, 0.0125 mmol, 1.0 eq.) and PMDETA (4.0 µL, 0.019 mmol, 1.5 eq.) were dissolved in DMSO (3.0 mL) and added to the reaction mixture. The reaction mixture was stirred at ambient temperature for 48 hours. Azido functionalized PS-resin (8.0 mg, 0.018 mmol) and ascorbic acid (4.4 mg, 0.025 mmol, 2.0 eq.) were added and the reaction mixture was stirred for additional 48 h. The resin was filtered off and the solution was dialyzed against deionized water for three days followed by lyophilization to afford Pull$_{17k}$-b-PEtOx$_{22k}$ (0.53 g, 0.015 mmol, 95% recovery M_n =

35200 g·mol^{-1}, pullulan standard in acetate buffer with 20% MeOH, Đ= 1.7) as a white powder.

Preparation of aqueous PEtOx-b-Pull block copolymer solutions for DLS investigations

The diblock copolymer solutions of different weight percentages for DLS investigations were prepared as follows. The block copolymers were precisely weighed into vials according to the final weight percentage of the solution. Millipore water was added and the mixture was shaken until the block copolymers were completely dissolved (see Table S4). The solutions were filtered with hydrophilic 0.45 µm syringe filters (Satorius CA filters) prior to DLS examination.

Characterization Methods

^{1}H and ^{13}C NMR spectra were recorded at ambient temperature at 400 MHz for ^{1}H and 100 MHz for ^{13}C with a Bruker Ascend400. Dynamic light scattering (DLS) and static light scattering (SLS) was performed using an ALV-7004 Multiple Tau Digital Correlator in combination with a CGS-3 Compact Goniometer and a HeNe laser (Polytec, 34 mW, λ = 633 nm at ϑ = 30° to 150° with steps of 10° for DLS and SLS). Sample temperatures were adjusted to 25 °C. Toluene was used as immersion liquid. Apparent hydrodynamic radii (R_{app}) have been determined from fitting autocorrelation functions by using REPES algorithm. Radii of gyration (R_g) were determined via SLS with ALV Stat ALV-5000 using a Guinier plot. Cryogenic scanning electronic microscopy (cryo SEM) was performed on a Jeol JSM 7500 F and the cryo-chamber from Gatan (Alto 2500). Size exclusion chromatography (SEC) for PEtOx was conducted in NMP (Fluka, GC grade) with 0.05 mol L^{-1} LiBr and BSME as internal standard at 70 °C using a column system by PSS GRAM 100/1000 column (8 x 300 mm, 7 µm particle size) with a PSS GRAM precolumn (8 x 50 mm) and a Shodex RI-71 detector and a poly(methyl methacrylate)

calibration with standards from PSS. Pullulan samples were analyzed in acetate buffer containing 20% MeOH at 25 °C using a PSS NOVEMA Max analytical system XL (pre column size 50 mm x 8 mm – 10 μm, main column size 300 mm x 8 mm - 10 μm) using a pullulan calibration with standards from PSS. Laser scanning confocal microscopy (LSCM) measurements were conducted with a Leica TCS SP5 (Wetzlar, Germany) confocal microscope, using a 63x (1.2 NA) water immersion objective. The dye stained samples were excited with a diode pumped solid-state laser at 561 nm and the emission bands were collected at 640 nm. Turbidimetry measurements to obtain the lower critical solution temperature (LCST) were conducted with a T70+ UV/Vis Spectrometer (PG Instruments Ltd) at a wavelength of 660 nm and a temperature control system consisting of a Peltier Temperature Controller PTC-2 and a Manson Switching Mode Power Supply 1-36VDC-10A. Typically, 0.5 wt.% solutions were investigated with a heating rate of 1 K min^{-1} and the transmission values were detected within a 5 second interval. Optical microscopy was performed on a Leica DVM6 digital microscope with a PLANAPO FOV 3.6 objective and a transmitted light adaptor by Leica (Germany). Remaining copper in polymer products were determined by inductively coupled plasma optical emission spectrophotometer (ICP-OES), and the measurement was performed on Perkin Elmer Optima 8000, calibrated with standard solutions. Fourier transform infrared (FT-IR) spectra were acquired on a Nicolet iS 5 FT-IR spectrometer.

RESULTS AND DISCUSSION

Synthesis of homo polymer building blocks

The Pull-*b*-PEtOx diblock copolymers were formed via CuAAc. Therefore, the individual Pull-alkyne and PEtOx-N$_3$ blocks were synthesized at the beginning. To allow self-assembly studies with respect to differences in block molecular masses, the molecular mass of Pull-alkyne blocks was varied. At first commercial pullulan precursor was

depolymerized under acidic conditions with specific reaction times to afford depolymerized pullulan with designed molecular mass. Next, the aldehyde endgroup of depolymerized pullulan was reacted with propargyl amine in a reductive amination reaction to obtain the alkyne functional pullulan building block. Thus pullulan-alkyne with M_{nSEC} according to pullulan standards ranging from 7900 to 38000 g mol^{-1} and Đ of 1.7 to 2.6 was synthesized (Table 1). Monomodal distributions were obtained. To investigate the success of alkyne functionalization ^{1}H NMR was conducted (Figure S1). Due to the overlap of the propargyl related signals with signals from the pullulan backbone, the alkyne addition could not be verified directly. Nevertheless, the signals corresponding to the α-glycosidic protons at 6.7 ppm and 6.3 ppm vanish, which is a strong indication of reductive amination taking place (Figure S2). The synthesis of the PEtOx-N$_3$ block was carried out via cationic ring-opening polymerization of 2-ethyl-2-oxazoline at 80 °C.[28] The azide functionalization was afforded via termination of the cationic chain ends with the azide anion.[50] The incorporation of an azide end group was verified via ^{1}H NMR displaying the methylene peaks adjacent to the azide group around 1.8 ppm and 3.7 ppm (Figure S3). The incorporation of azide endgroups was further confirmed via FTIR spectroscopy (Figure S4). The N-N stretching band was observed at 2100 cm^{-1}. Moreover, the molecular mass distribution of PEtOx-N$_3$ was determined via SEC analysis against poly(methyl methacrylate) calibration in NMP. A monomodal distribution with Đ of 1.24 was obtained and the M_{nSEC} estimated to be 22200 g mol^{-1} (Figure 1). Next, the obtained alkyne and azide functionalized building blocks were conjugated via CuAAc.

Synthesis of Pull-*b*-PEtOx block copolymers

The conjugation of the building blocks was performed via CuAAc with CuSO$_4$ and ascorbic acid as reagents. To ensure complete reaction

an excess of the pullulan block was added and after the reaction an azide functionalized resin was added to bind unreacted Pullulan-alkyne for easy removal. DHBC formation was studied via ^{1}H NMR in order to confirm the presence of both polymer blocks (Figure 1 and S5-S9). Peaks corresponding to protons from both blocks are visible, e.g. the anomeric protons of the pullulan backbone at 5.0 ppm and the side-chain methyl peaks of $PEtOx_{22k}$ at 0.9 ppm. Furthermore, the integral ratio of the different blocks was determined via ^{1}H NMR, which is in-line with the expectations from the estimated DPs of the individual blocks.
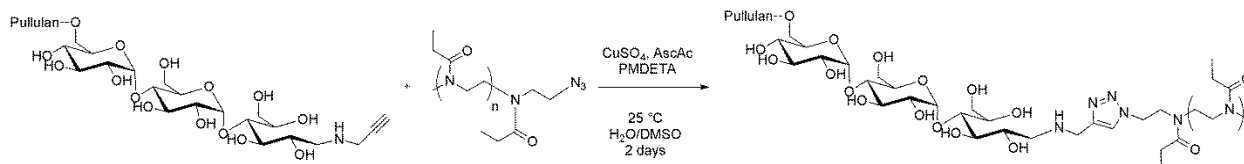
SCHEME 2 Overview of Pull-*b*-PEtOx block copolymer synthesis.

TABLE 1 Properties of the utilized polysaccharides and Pull-*b*-PEtOx block copolymers.

Polymer	M_{nSEC} [g mol^{-1}][a]	Đ[a]	Block copolymer	M_{nSEC} [g mol^{-1}][a]	Đ[a]	molar ratio Pull/PEtOx[b]
Pull-alkyne$_{7.9k}$	7900	2.9	Pull$_{7.9k}$-*b*-PEtOx$_{22k}$	21300	1.9	0.21/0.79
Pull-alkyne$_{14k}$	16000	1.8	Pull$_{16k}$-*b*-PEtOx$_{22k}$	27400	1.7	0.37/0.63
Pull-alkyne$_{19k}$	17000	1.9	Pull$_{17k}$-*b*-PEtOx$_{22k}$	35200	1.7	0.38/0.62
Pull-alkyne$_{24k}$	24000	2.3	Pull$_{24k}$-*b*-PEtOx$_{22k}$	28700	1.9	0.44/0.56
Pull-alkyne$_{30k}$	30000	2.4	Pull$_{30k}$-*b*-PEtOx$_{22k}$	22700	2.0	0.51/0.49
Pull-alkyne$_{38k}$	38000	2.7	Pull$_{38k}$-*b*-PEtOx$_{22k}$	36100	2.6	0.58/0.42

a) obtained via SEC in acetate buffer containing 20% methanol against pullulan standards, b) determined via ^{1}H NMR in DMSO-d$_6$

Moreover, the block copolymer products were analyzed via SEC in acetate buffer containing 20% methanol (Figure 1 and S10-S14). For Pull$_{7.9k}$-*b*-PEtOx$_{22k}$, Pull$_{16k}$-*b*-PEtOx$_{22k}$ and Pull$_{17k}$-*b*-PEtOx$_{22k}$ a significant shift of the molecular mass distribution towards lower retention time was evident compared to the starting materials as well as the mixture of starting materials. Moreover, a shift in M_{nSEC} is calculated from pullulan calibration. Interestingly, in the case of Pull$_{24k}$-*b*-PEtOx$_{22k}$, Pull$_{30k}$-*b*-PEtOx$_{22k}$ and Pull$_{38k}$-*b*-PEtOx$_{22k}$ the elution trace of the block copolymer resembles the trace of the pullulan starting material. Therefore, the estimated molecular mass M_{nSEC} from pullulan calibration does not match the expectations as well.

Nevertheless, NMR results state the presence of both polymer blocks and the molar ratio obtained via NMR integration matches the expectations. Furthermore, mono modal distributions are obtained in SEC, no PEtOx starting material is observed and excess pullulan-alkyne should have reacted with the resin. Therefore, the unexpected elution and M_{nSEC} for the three samples with high pullulan content might be due to a chromatographic effect, e.g. interactions with the column. The block copolymer products were studied via FTIR spectroscopy as well (Figure S4). In the product no azide band is present, which is another indication of a successful CuAAc reaction. In order to assess the utilization of the polymers

for future applications residual copper contents were measured via inductively coupled plasma optical emission spectrometry (ICP-OES) for some block copolymer samples. A residual amount of 0.98-1.37 mg/g of copper was found (Table S3). Certainly, for biomedical applications the block conjugation method has to be changed.
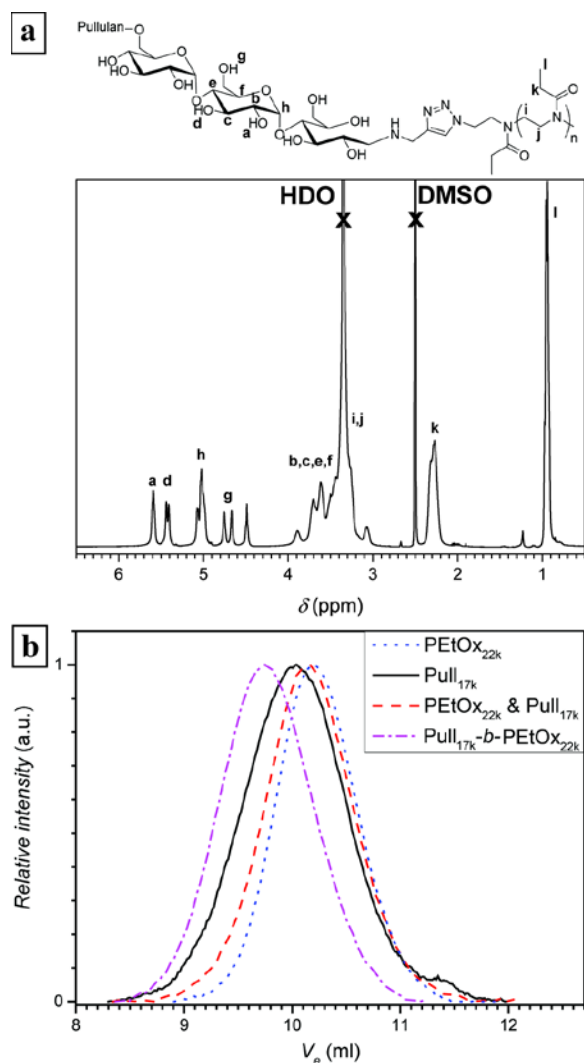
Figure 1 Analysis of Pull$_{17k}$-b-PEtOx$_{22k}$ block copolymers: a) ^{1}H-NMR spectrum measured at 25 °C in DMSO-d$_6$ and b) SEC traces measured in acetate buffer containing 20% methanol.

PEtOx is well-known for its thermo response, which is indicated by a coil-to-globule transition at the lower critical solution temperature (LCST). Therefore, turbidimetry was studied to ensure no coil-to-globule transition of the PEtOx block takes place in the investigated temperature range during the self-assembly process. It could be shown that no phase transition occurs from 20 °C to 60 °C and thus thermo response effects in the self-assembly studies can be excluded (Figure S15). Visual assessment showed a LCST of 82 °C for PEtOx-N$_3$, while for the block copolymer a LCST of 87 °C was observed (Figure S16). The shift towards increased temperatures is in line with the addition of a hydrophilic block and another hint towards block copolymer formation.

Self-assembly of Pull-b-PEtOx block copolymers

After confirmation of Pull-b-PEtOx block copolymer synthesis, self-assembly of the DHBC in aqueous solution was probed. Therefore, the block copolymers were dissolved in the pre-determined amount of water and the mixture shaken until the solid was dissolved. In order to investigate the formation of self-assembled structures in aqueous solution, DLS was utilized (Table S4). The obtained particle size distributions show a significant influence of the Pullulan molecular mass on the self-assembly behavior at a scattering angle of 90° (Table 2 and Figure 2).

In all cases bimodal particle size distributions are observed (Figure 2 and S14). Small particles with R_{app} around 5 nm are obtained for all cases except of Pull$_{38k}$-b-PEtOx$_{22k}$, where a particle R_{app} of 8.0 nm is calculated (Table 2). The small particles correspond to a fast diffusing species that shows sizes in the range of small micellar aggregates or single block copolymer chains. The slower diffusion species have R_{app} in the range of 161 to 252 nm (Table 2). In comparison with the corresponding homopolymers, e.g. Pull$_{16k}$ and PEtOx$_{22k}$, a significant difference is obvious (Figure S15). First of all, the homopolymers do not show any species with R_{app} above 180 nm. While PEtOx$_{22k}$ does not show any large species, Pull$_{16k}$ shows homopolymer aggregates with R_{app} around 180 nm that is still significantly smaller than the

smallest block copolymer particle R_{app}. Secondly, the observed R_{app} of $PEtOx_{22k}$ (6.8 nm) and the fast diffusing species of $Pull_{16k}$ (6.9 nm) is in the range of 3-10 nm, which points to the conclusion that the small diffusion species in block copolymers investigations are due to single block copolymer chains. Moreover, from the particle size distributions for different block copolymer samples a significant concentration dependence of the self-assembly can be concluded (Figure 2 and S14). As expected, at higher DHBC concentrations an increased amount of self-assembled particles are formed. Nevertheless, even at concentrations around 1 wt.% a significant amount of particles is formed, e.g. an abundance of 95% polymer particles in intensity for $Pull_{17k}-b-PEtOx_{22k}$. Moreover, at 0.1 wt.% particle structures are found to a similar extent, e.g. an abundance of

10% free polymer chains in intensity for $Pull_{17k}-b-PEtOx_{22k}$. Nevertheless, the concentration dependence is relying significantly on the polymer block volume ratios as discussed in the preceding section. Furthermore, the average observed particle radius R_{app} shifts with concentration. While the apparent radius is similar for concentrations of 0.5 wt.% and 1 wt.% for all samples, a significant shift towards lower radii is observed upon dilution to 0.1 wt.%, e.g. from 221.8 nm to 185 nm in the case of $Pull_{17k}-b-PEtOx_{22k}$ (Figure 2). The DLS results discussed here are based on intensity weighted distributions. As larger particles show significantly enhanced scattering they are overexpressed in intensity weighted distributions. Therefore, abundances form intensity weighted distributions have to be considered with care.

TABLE 2 DLS intensity weighted results from Pull-b-PEtOx block copolymers.

Polymer	R_{app} [nm][a]	R_{app} [nm][a]	Abundance[b]
	fast diffusing species	slow diffusing species	slow/fast diffusing species
$Pull_{7.9k}-b-PEtOx_{22k}$	5.3	161.4	0.05/0.93
$Pull_{16k}-b-PEtOx_{22k}$	5.2	195.1	0.15/0.85
$Pull_{17k}-b-PEtOx_{22k}$	5.7	221.8	0.05/0.95
$Pull_{24k}-b-PEtOx_{22k}$	5.1	179.6	0.09/0.91
$Pull_{30k}-b-PEtOx_{22k}$	5.4	170.0	0.05/0.95
$Pull_{38k}-b-PEtOx_{22k}$	8.0	252.2	0.10/0.90

a) obtained via DLS at a scattering angle of 90° at a temperature of 25 °C and a concentration of 1.0 wt.% intensity weighted, b) intensity weighted at a concentration of 1.0 wt.%

In order to get a deeper insight into the formed structures in solution, SLS was investigated in the case of $Pull_{17k}-b-PEtOx_{22k}$ (Figure S19 and Table S5). A R_g value of 106.1 nm was found, which is a rather low value compared to the R_{app} value of 222 nm. The quotient of both radii R_g/R_{app} is with the value of 0.48 lower than the theoretical value for a dense sphere. Probably the R_g value is underestimated due to the presence of fast diffusing block copolymer

chains, which is also reflected in the low M_w of the self-assemblies (Table S5). Furthermore, the R_{app} value of 222 nm in the case of $Pull_{17k}-b-PEtOx_{22k}$ states that the formed self-assembled structure is too large to be a micellar aggregate as the contour length of $Pull_{17k}-b-PEtOx_{22k}$ is around 147 nm (117*0.57 nm + 224*0.36 nm).[25,51] The formation of a vesicular structure cannot be excluded. Nevertheless, the presence of significant amounts of fast diffusing

species prevents the final elucidation of the matter. Therefore, the self-assembled aggregates are rather called nanoparticles.

Additionally, effects of external stimuli on the self-assembly was probed (Figure S20). Changes in pH to 5 or 9 as well as utilization of 2 M NaCl solution did not lead to changes in the particle size distributions of $Pull_{30k}$-b-$PEtOx_{22k}$. Nevertheless, utilization of 2 M urea solution led to slight increased abundance of self-assembled particles. A similar effect was observed, when 0.04 wt.% of pluronics (Pluronic P-123) were added to the solution, although a significant shift to lower R_{app} (114 nm) of the slow diffusing species was observed.

Particle formation can be visualized via cryo SEM as well as LSCM imaging. In cryo SEM mostly spherical aggregates are visible consisting of Pull-b-PEtOx DHBCs at a concentration of 0.5 wt.% (Figure 3 and S21-S22). The observed particles diameters resemble the results from DLS measurements of around 200-300 nm but also a smaller fraction of larger particles is visible. Moreover, imaging via LSCM shows spherical particles as well (Figure 4 and S20). Particle sizes of 500 nm to 1.5 µm are observed. Smaller particles are hardly to find due to the limited resolution of LSCM as well as particle motion. Overall, the microscopy results support the findings from DLS that state particle formation of Pull-b-PEtOx in aqueous solution.
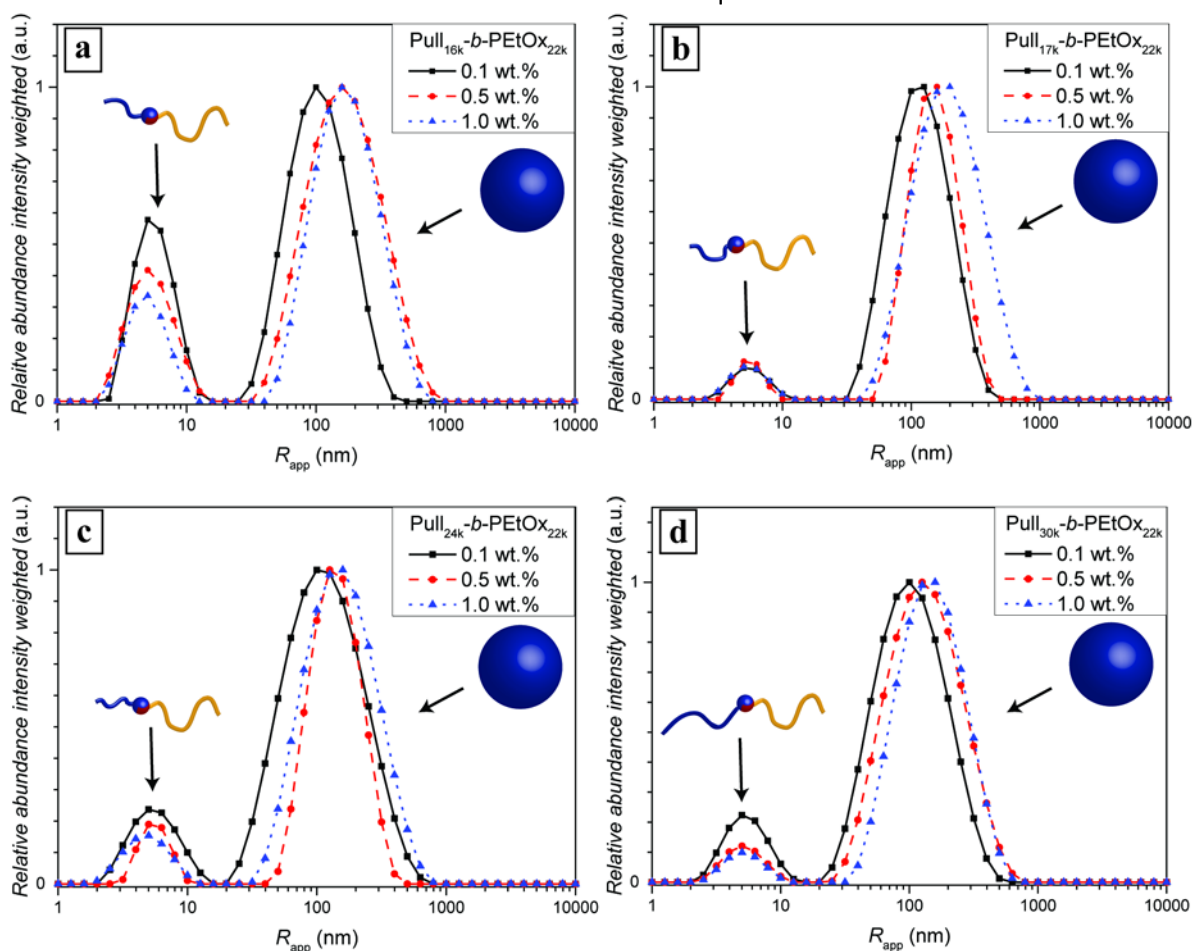
FIGURE 2 DLS investigations of Pull-b-PEtOx self-assembly affording intensity weighted particle size distribution at different concentrations calculated from scattering at an angle of 90°.
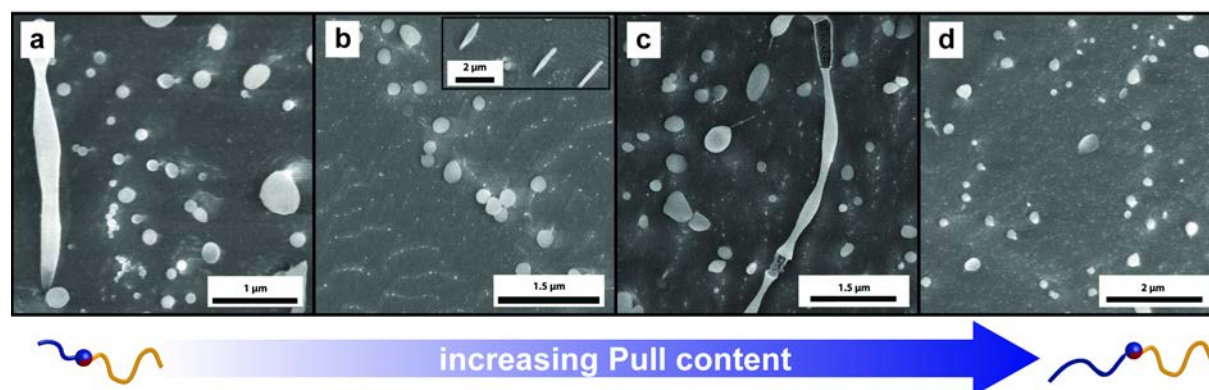
FIGURE 3 Cryo SEM imaging of Pull-*b*-PEtOx self-assembled structures at a concentration of 0.5 wt.%: a) Pull$_{16k}$-*b*-PEtOx$_{22k}$, b) Pull$_{17k}$-*b*-PEtOx$_{22k}$, c) Pull$_{24k}$-*b*-PEtOx$_{22k}$ and d) Pull$_{30k}$-*b*-PEtOx$_{22k}$.

As shown by Brosnan et al., at high concentration giant DHBC vesicles are accessible. Therefore, self-assembly formation at high concentrations, namely 20 wt.%, was studied. Certainly, light scattering is not a suitable technique to study the self-assembly at very high concentrations. Nevertheless, the formation of spherical structures from Pull$_{24k}$-*b*-PEtOx$_{22k}$ could be imaged via optical microscopy (Figure 4). Spherical structures with diameters around 1 µm are visible that correspond to particles of significant size.
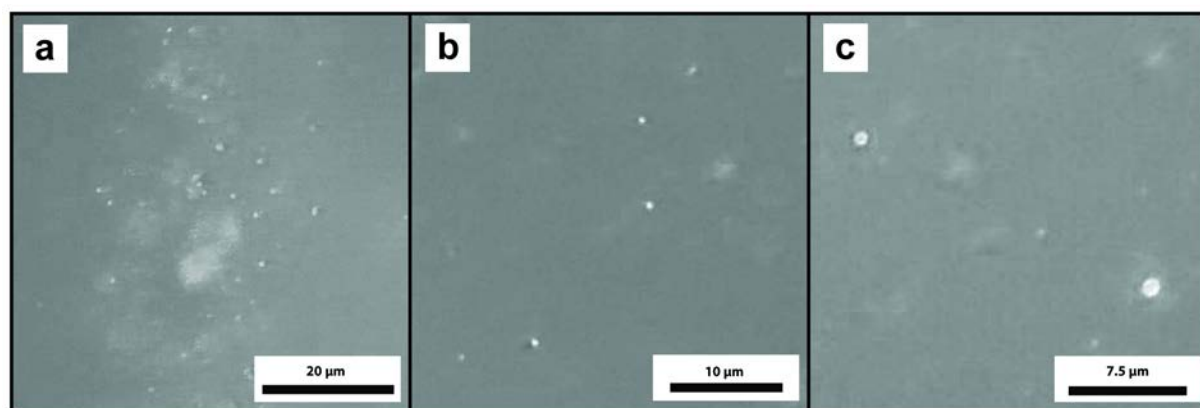
FIGURE 4 Optical microscopy imaging of Pull$_{24k}$-*b*-PEtOx$_{22k}$ self-assembled giant vesicular structures at a concentration of 20 wt.% and 25 °C.

The formation of aqueous multi-phase systems can be utilized to gain a preview on the self-assembly process. Whitesides and coworkers showed macroscopic demixing of aqueous solutions of PEtOx and Dextran, which is similar to Pull.[49] Therefore, microscopic self-assembly of a DHBC driven by the incompatibility of the individual blocks in water is possible. A hint towards the reason for the formation of self-assembled DHBC structures can be obtained via a comparison of the second virial coefficient A_2 of the individual blocks. From the literature A_2 values around 8.7×10^4 cm^3 mol g^{-2} can be found for PEtOx with a molecular mass of 12000 g mol^{-1} at 30 °C.[52] For Pullulan A_2 ranging from 4.9 to 13.2×10^4 cm^3 mol g^{-2} in the molecular mass range from 10000 to 50000 g mol^{-1} can be found for aqueous solutions at ambient temperature.[53] The significantly different A_2 values indicate a significantly different

interaction of the respective blocks with water, which is one reason for the formation of self-assembled DHBC structures. A similar conclusion can be drawn from the demixing of homopolymer solutions (Scheme 1a) that shows the incompatibility of Pull and PEtOx in water at increased concentrations. Furthermore, it was previously shown that thermoresponsive polymer blocks lead to efficient self-assemblies, although the self-assembly takes place far beyond the cloud point of the respective blocks.[31] The LCST effect is connected to water-polymer interactions and thus might be a hint towards efficient DHBC self-assembly without utilization of the thermo trigger. Moreover, due to the LCST behavior of PEtOx it can be assumed that the PEtOx block is the less hydrophilic block in the Pull-*b*-PEtOx block copolymer and thus preferentially on the outside of the self-assembled structures. The assumption is further supported by zeta potential measurements that show a similar zeta potential for the block copolymer and Pull homopolymer (Table S6).

Overall, DHBC particle formation can be stated and the extent of particle formation is depending on polymer concentration as expected. Furthermore, particle formation is depending on the ratios of the utilized blocks, which will be discussed in the next section.

Effect of block ratio on self-assembly of Pull-*b*-PEtOx block copolymers

Taking all investigated particle size distributions into account, the abundance of self-assembled structures is most significant in the case of Pull$_{17k}$-*b*-PEtOx$_{22k}$ (Figure 2). A maximum of self-assembled structures is found for Pull$_{17k}$-*b*-PEtOx$_{22k}$, while for higher volume fractions and lower volume fractions of the pullulan block less abundance of self-assembled structures is observed. Thus, the measurement clearly points to the conclusion that there is an optimum ratio of pullulan to PEtOx blocks for the formation of DHBC self-assemblies. Moreover, Pull$_{17k}$-*b*-PEtOx$_{22k}$ shows no significant change in the

abundance of small particles with dilution. For the other cases dilution leads to increased amounts of small species with R_{app} around 5 nm. Interestingly, the optimum molar block ratio is around 0.38/0.62 Pull/PEtOx (Figure S24). Obtained particle sizes also show strong dependence on the designed block ratios. Analog to the abundance of self-assembled structures, a maximum of the particles size is found for Pull$_{17k}$-*b*-PEtOx$_{22k}$ that shows a R_{app} of 221.8. The maximum points again to the conclusions that there is an optimum block ratio for the formation of self-assembled structures. Similar to the case of fast diffusing species, Pull$_{38k}$-*b*-PEtOx$_{22k}$ is an exception with a R_{app} of 252.2 nm that is significantly larger than the size of Pull$_{17k}$-*b*-PEtOx$_{22k}$ based particles and might be due to the formation of more complex membrane structures.

Cryo SEM imaging shows the formation of spherical particles at a concentration of 2.5 wt.% in all cases (Figure 3 and S21-S22). Nevertheless in the case of Pull$_{30k}$-*b*-PEtOx$_{22k}$ aggregates of spherical particles connected via polymer slings are found (Figure S21). In the case of Pull$_{7.9k}$-*b*-PEtOx$_{22k}$ particles with less defined surface are visible (Figure S21). Imaging via LSCM shows spherical particles regardless of pullulan chain length (Figure 5 and S23).

Moreover, cryo SEM investigations show formation of non-spherical worm-like aggregates in the case of some block ratios, namely Pull$_{16k}$-*b*-PEtOx$_{22k}$, Pull$_{17k}$-*b*-PEtOx$_{22k}$ and Pull$_{24k}$-*b*-PEtOx$_{22k}$, albeit to a low extent (Figure 3, Figure S21-S22). Similarly, in LSCM anisotropic as well as spherical particles are visible (Figure 5a). Nevertheless, only minor amounts of anisotropic particles are formed, which is also evident in angle dependent DLS measurements. The plot of $\Gamma\ q^{-1}$ against q^2 for the slowly diffusing species shows almost a horizontal line that clearly indicates the formation of spherical particles (Figure S25).[54] Although non-spherical particles are observed in the range of pullulan block molar masses between 14000 g mol^{-1} and 24000 g mol^{-1} there

is no indication that an increased fraction of non-spherical particles can be formed via changes in the molar mass of the pullulan block in that range. Nevertheless, the observed effect of non-spherical particle formation is unprecedented and certainly opens up new opportunities for future research, e.g. studies for combinations with other hydrophilic polymers or experimental conditions to induce non-spherical DHBC particle formation. While light scattering did not finally answer whether hollow particles or dense particles are formed

in the self-assembly process, cryo SEM suggests that actually hollow particles are formed as visible in Figure 3c and S22. Broken tubular particles seem to be hollow, which indicates the formation of wormlike vesicular structures.

Overall, variations in the molar ratio of the different blocks lead to significant changes in the formed assemblies especially when self-assembly efficiency is considered. Nevertheless, the observed changes do not resemble the structural possibilities amphiphilic block copolymers offer.[1]
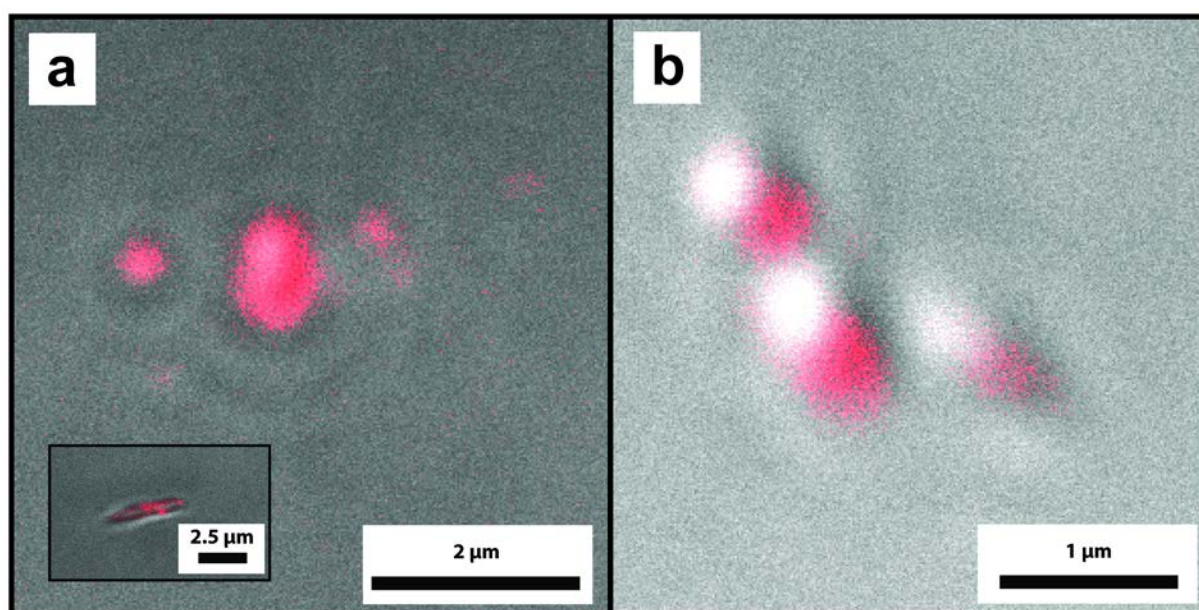
FIGURE 5 LSCM imaging of Pull-*b*-PEtOx self-assembled structures at a concentration of 2.5 wt.%: a) Pull$_{16k}$-*b*-PEtOx$_{22k}$ and b) Pull$_{17k}$-*b*-PEtOx$_{22k}$.

CONCLUSIONS

The self-assembly of novel DHBC Pull-*b*-PEtOx in water was investigated. The block copolymer was formed from modified biomacromolecule Pull and biocompatible PEtOx in a modular CuAAc conjugation. Moreover, the molecular weight of the Pull block was varied in order to study the dependency of the self-assembly behavior from molecular weight. Spherical self-assembled structures were found in aqueous solution with sizes between 300 and 500 nm

without the application of external triggers as determined via DLS as well as SLS. Moreover, the formed structures could be visualized via cryo SEM and LSCM. A significant influence of the molar content of the individual blocks was observed with an optimum around 40 mol % of the Pull block. At high concentrations (20 wt.%) vesicular structures with sizes around 1-2 μm were observed via optical microscopy. Overall, self-assembled structures from completely water-soluble biocompatible polymers are

formed that might find biomedical applications or as container for nano reactors in the future.

ACKNOWLEDGEMENTS

REFERENCES AND NOTES

1. M. Antonietti, S. Förster. *Adv. Mater.* **2003**, *15*, 1323-1333.

2. D. E. Discher, A. Eisenberg. *Science* **2002**, *297*, 967-973.

3. B. L. Mui, H. G. Döbereiner, T. D. Madden, P. R. Cullis. *Biophys. J.* **1995**, *69*, 930-941.

4. F. Meng, Z. Zhong, J. Feijen. *Biomacromolecules* **2009**, *10*, 197-209.

5. G. Yu, W. Yu, L. Shao, Z. Zhang, X. Chi, Z. Mao, C. Gao, F. Huang. *Adv. Funct. Mater.* **2016**, *26*, 8999-9008.

6. L. Schoonen, J. C. M. van Hest. *Adv. Mater.* **2016**, *28*, 1109-1128.

7. J. Gaitzsch, X. Huang, B. Voit. *Chem. Rev.* **2016**, *116*, 1053-1093.

8. S. Haas, N. Hain, M. Raoufi, S. Handschuh-Wang, T. Wang, X. Jiang, H. Schönherr. *Biomacromolecules* **2015**, *16*, 832-841.

9. C. Houga, J. Giermanska, S. Lecommandoux, R. Borsali, D. Taton, Y. Gnanou, J.-F. Le Meins. *Biomacromolecules* **2009**, *10*, 32-40.

10. J. P. Jain, N. Kumar. *Biomacromolecules* **2010**, *11*, 1027-1035.

11. F. Li, F. A. de Wolf, A. T. M. Marcelis, E. J. R. Sudhölter, M. A. Cohen Stuart, F. A. M. Leermakers. *Angew. Chem., Int. Ed.* **2010**, *49*, 9947-9950.

12. L. K. E. A. Abdelmohsen, D. S. Williams, J. Pille, S. G. Ozel, R. S. M. Rikken, D. A. Wilson, J. C. M. van Hest. *J. Am. Chem. Soc.* **2016**, *138*, 9353-9356.

13. K. T. Kim, J. Zhu, S. A. Meeuwissen, J. J. L. M. Cornelissen, D. J. Pochan, R. J. M. Nolte, J. C. M. van Hest. *J. Am. Chem. Soc.* **2010**, *132*, 12522-12524.

14. M. J. Derry, L. A. Fielding, S. P. Armes. *Prog. Polym. Sci.* **2016**, *52*, 1-18.

15. R. S. M. Rikken, H. Engelkamp, R. J. M. Nolte, J. C. Maan, J. C. M. van Hest, D. A. Wilson, P. C. M. Christianen. *Nat. Commun.* **2016**, *7*, 12606.

16. A. A. Reinecke, H.-G. Döbereiner. *Langmuir* **2003**, *19*, 605-608.

17. L. Zhang, K. Yu, A. Eisenberg. *Science* **1996**, *272*, 1777-1779.

18. S. M. Brosnan, H. Schlaad, M. Antonietti. *Angew. Chem., Int. Ed.* **2015**, *54*, 9715-9718.

19. A. E. Smith, X. Xu, C. L. McCormick. *Prog. Polym. Sci.* **2010**, *35*, 45-93.

20. Y. Zhou, K. Jiang, Q. Song, S. Liu. *Langmuir* **2007**, *23*, 13076-13084.

21. A. F. Hirschbiel, B. V. K. J. Schmidt, P. Krolla-Sidenstein, J. P. Blinco, C. Barner-Kowollik. *Macromolecules* **2015**, *48*, 4410-4420.

22. B. V. K. J. Schmidt, M. Hetzer, H. Ritter, C. Barner-Kowollik. *Macromol. Rapid Commun.* **2013**, *34*, 1306-1311.

23. B. V. K. J. Schmidt, C. Barner-Kowollik. *Polym. Chem.* **2014**, *5*, 2461-2472.

24. A. Taubert, E. Furrer, W. Meier. *Chem. Commun.* **2004**, 2170-2171.

25. O. Casse, A. Shkilnyy, J. Linders, C. Mayer, D. Häussinger, A. Völkel, A. F. Thünemann, R. Dimova, H. Cölfen, W. Meier, H. Schlaad, A. Taubert. *Macromolecules* **2012**, *45*, 4772-4777.

26. F. Ke, X. Mo, R. Yang, Y. Wang, D. Liang. *Macromolecules* **2009**, *42*, 5339-5344.

27. J. Willersinn, M. Drechsler, M. Antonietti, B. V. K. J. Schmidt. *Macromolecules* **2016**, *49*, 5331-5341.

28. J. Willersinn, B. V. K. J. Schmidt. *Polymers* **2017**, *9*, 293.

29. H. Park, S. Walta, R. R. Rosencrantz, A. Korner, C. Schulte, L. Elling, W. Richtering, A. Boker. *Polym. Chem.* **2016**, *7*, 878-886.

30. J. O. Kim, A. V. Kabanov, T. K. Bronich. *J. Controlled Release* **2009**, *138*, 197-204.

31. J. Willersinn, A. Bogomolova, M. Brunet Cabré, B. V. K. J. Schmidt. *Polym. Chem.* **2017**, *8*, 1244-1254.

32. H. Schlaad, C. Diehl, A. Gress, M. Meyer, A. L. Demirel, Y. Nur, A. Bertin. *Macromol. Rapid Commun.* **2010**, *31*, 511-525.

33. C. Diehl, H. Schlaad. *Chem. - Eur. J.* **2009**, *15*, 11469-11472.

34. A. Mero, G. Pasut, L. D. Via, M. W. M. Fijten, U. S. Schubert, R. Hoogenboom, F. M. Veronese. *J. Controlled Release* **2008**, *125*, 87-95.

35. T. Rudolph, M. v. d. Lühe, M. Hartlieb, S. Norsic, U. S. Schubert, C. Boisson, F. D'Agosto, F. H. Schacher. *ACS Nano* **2015**, *9*, 10085-10098.

36. K. Knop, R. Hoogenboom, D. Fischer, U. S. Schubert. *Angew. Chem., Int. Ed.* **2010**, *49*, 6288-6308.

37. N. Adams, U. S. Schubert. *Adv. Drug Delivery Rev.* **2007**, *59*, 1504-1520.

38. R. Luxenhofer, A. Schulz, C. Roques, S. Li, T. K. Bronich, E. V. Batrakova, R. Jordan, A. V. Kabanov. *Biomaterials* **2010**, *31*, 4972-4979.

39. S. Cheon Lee, C. Kim, I. Chan Kwon, H. Chung, S. Young Jeong. *J. Controlled Release* **2003**, *89*, 437-446.

40. R. Hoogenboom, H. M. L. Thijs, M. J. H. C. Jochems, B. M. van Lankvelt, M. W. M. Fijten, U. S. Schubert. *Chem. Commun.* **2008**, 5758-5760.

41. C. Diehl, H. Schlaad. *Macromol. Biosci.* **2009**, *9*, 157-161.

42. V. Ďorďovič, M. Uchman, K. Procházka, A. Zhigunov, J. Pleštil, A. Nykänen, J. Ruokolainen, P. Matějíček. *Macromolecules* **2013**, *46*, 6881-6890.

43. W. M. Kulicke, T. Heinze. *Macromol. Symp.* **2005**, *231*, 47-59.

44. M. E. Gounga, S. Y. Xu, Z. Wang, W. G. Yang. *J. Food Sci.* **2008**, *73*, E155-E161.

45. K.-C. Cheng, A. Demirci, J. M. Catchmark. *Appl. Microbiol. Biotechnol.* **2011**, *92*, 29-44.

46. H. C. Kolb, M. G. Finn, K. B. Sharpless. *Angew. Chem., Int. Ed.* **2001**, *40*, 2004-2021.

47. C. Barner-Kowollik, F. E. Du Prez, P. Espeel, C. J. Hawker, T. Junkers, H. Schlaad, W. Van Camp. *Angew. Chem., Int. Ed.* **2011**, *50*, 60-62.

48. J. F. Lutz. *Angew. Chem., Int. Ed.* **2007**, *46*, 1018-1025.

49. C. R. Mace, O. Akbulut, A. A. Kumar, N. D. Shapiro, R. Derda, M. R. Patton, G. M. Whitesides. *J. Am. Chem. Soc.* **2012**, *134*, 9094-9097.

50. G. Volet, T.-X. Lav, J. Babinot, C. Amiel. *Macromol. Chem. Phys.* **2011**, *212*, 118-124.

51. I. M. Neelov, D. B. Adolf, T. C. B. McLeish, E. Paci. *Biophys. J.* **2006**, *91*, 3579-3588.

52. F. P. Chen, A. E. Ames, L. D. Taylor. *Macromolecules* **1990**, *23*, 4688-4695.

53. K. Kawahara, K. Ohta, H. Miyamoto, S. Nakamura. *Carbohydr. Polym.* **1984**, *4*, 335-356.

54. J.-F. Gohy, S. K. Varshney, R. Jérôme. *Macromolecules* **2001**, *34*, 3361-3366.